

A Hydrodynamic Study of Stellar Wind Accretion in S-type Symbiotic Stars

UAI 2019. 11. 03 - 09, XVI LARIM 2019



Young-Min Lee¹, Hyosun Kim² and Hee-Won Lee¹
[ymlee9211.weebly.com]¹ Sejong University, ²KASI

1. Introduction

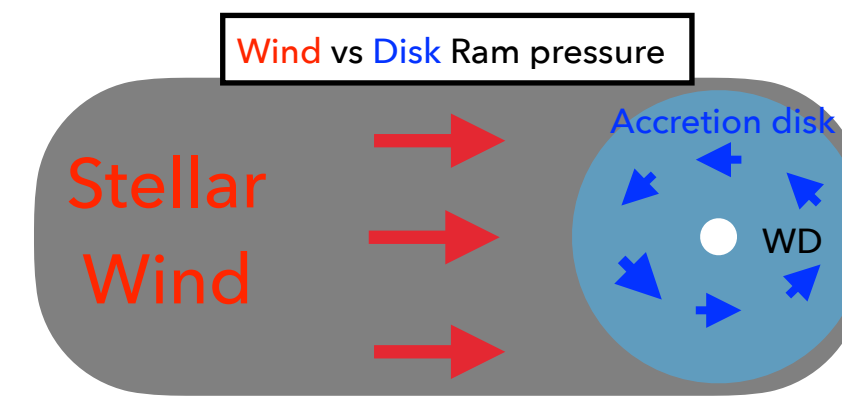
Symbiotic Stars

- Classified into S(stellar)-type & D(dusty)-type.
- Composed of RGB (S-type) or AGB (D-type) + White dwarf.
- Orbital periods range from a few years(S-type) to several decades (D-type).
- Mass transfer from Giant to WD via a slow stellar wind.
- Candidate of Type Ia SNe progenitors.
- Hydrodynamic simulations are required to elucidate accretion processes in Symbiotic Stars.



Formation of an accretion disk

- Hydrodynamical studies are essential in order to find detailed properties and the formation of an accretion disk in symbiotic stars.
- Fixing the pre-bow shock density, we focus on the role of ram pressure of the stellar wind flow at the outer boundary of the accretion disk.



First 3-D HD Simulations for Wind Accreting binary (Theuns & Jorissen 1993)

Formation of Accretion Disk

Formation of Accretion Disk & Disk evolution (Mastrodomos & Morris 1998) (Huarte-Espinoza et al. 2013) (Chen et al. 2017)

Estimation of Accretion Rates

Estimation of Accretion Rates & Mass Transfer (Mohamed & Polesiadowski 2007) (de Val-Borro et al. 2017)

Orbital Evolution

Orbital Evolution, Angular Momentum Loss (Nagae et al. 2004) (Jahanara et al. 2005) (Saladino et al. 2018)

2. Numerical Ingredients

FLASH4

Continuity Equation

$$\frac{\partial \rho}{\partial t} + \nabla \cdot (\rho \mathbf{u}) = 0$$

Momentum Equation

$$\rho \left[\frac{\partial \mathbf{u}}{\partial t} + (\mathbf{u} \cdot \nabla) \mathbf{u} \right] = -\nabla P - \rho \nabla \Phi$$

Energy Equation

$$\frac{\partial E}{\partial t} + \nabla \cdot [(E + P)\mathbf{u}] = -\rho \dot{Q}$$

Accretion Sink

if $(E_{\text{int}} + E_{\text{kin}} < E_{\text{grav}})$ & $(|\bar{\Gamma}| < r_{\text{sink}})$ & $(\rho > \rho_{\text{thres}})$

Simulation Model	a [au]	M ₁ [M _⊙]	M ₂ [M _⊙]	V _w [km s ⁻¹]	V _∞ [km s ⁻¹]	V ₂ [km s ⁻¹]	Ṁ [M _⊙ yr ⁻¹]
A2V9M1	2	1.5	0.6	9	14.7	21.8	10 ⁻⁷
A2V18M1	2	1.5	0.6	18	20.6	21.8	2 × 10 ⁻⁷
A4V5M1	4	1.5	0.6	5	13.2	15.4	10 ⁻⁷
A4V10M1 & 2	4	1.5	0.6	10	15.3	15.4	2 × 10 ⁻⁷

Pre-bow shock density

$$\rho_0 = \dot{M} / 4\pi r^2 v_w$$

Gravitational Potential

$$\Phi = -\frac{GM_1(1-f)}{\sqrt{(r-r_1)^2 + r_{\text{soft1}}^2}} - \frac{GM_2}{\sqrt{(r-r_2)^2 + r_{\text{soft2}}^2}}$$

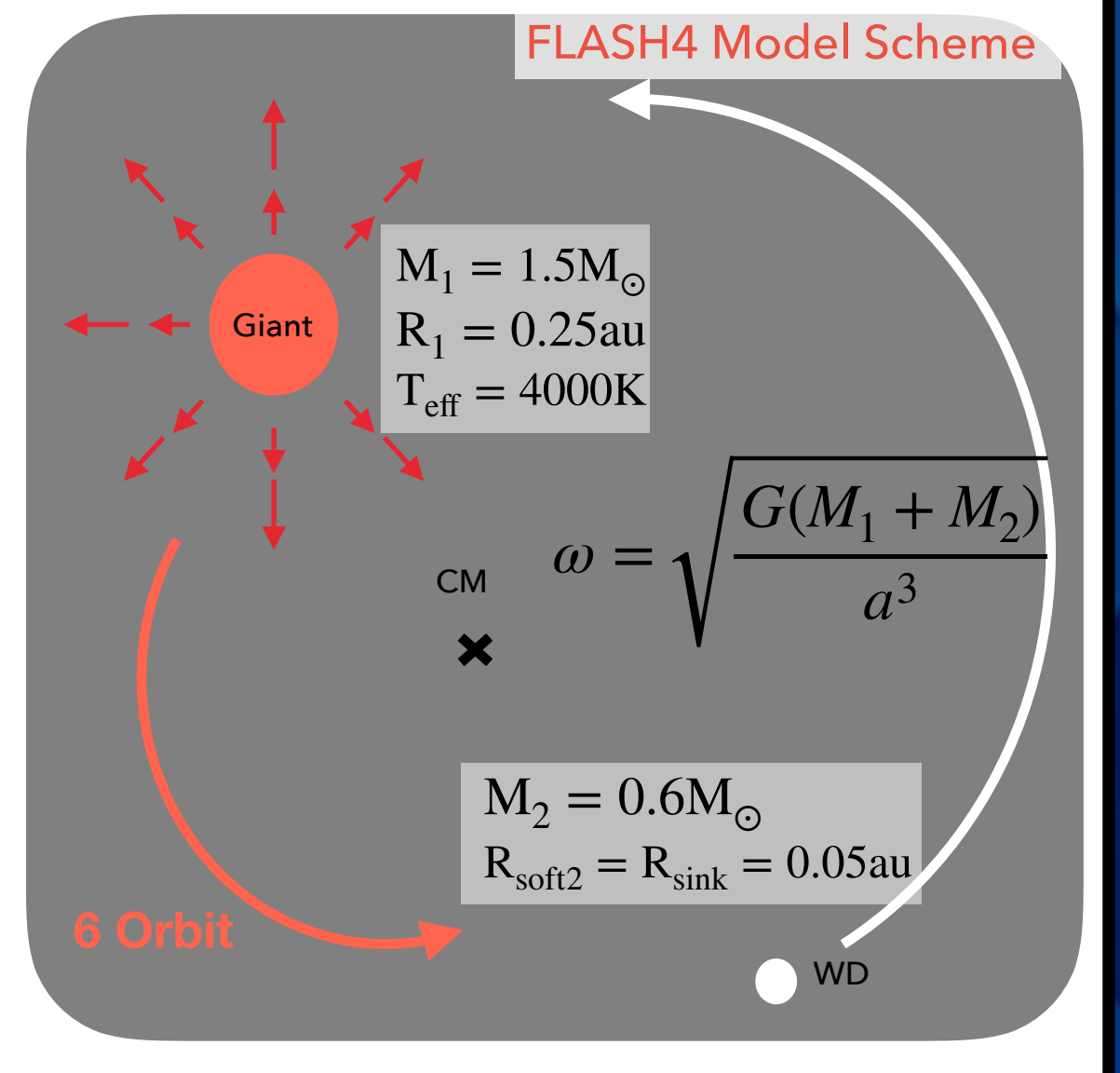
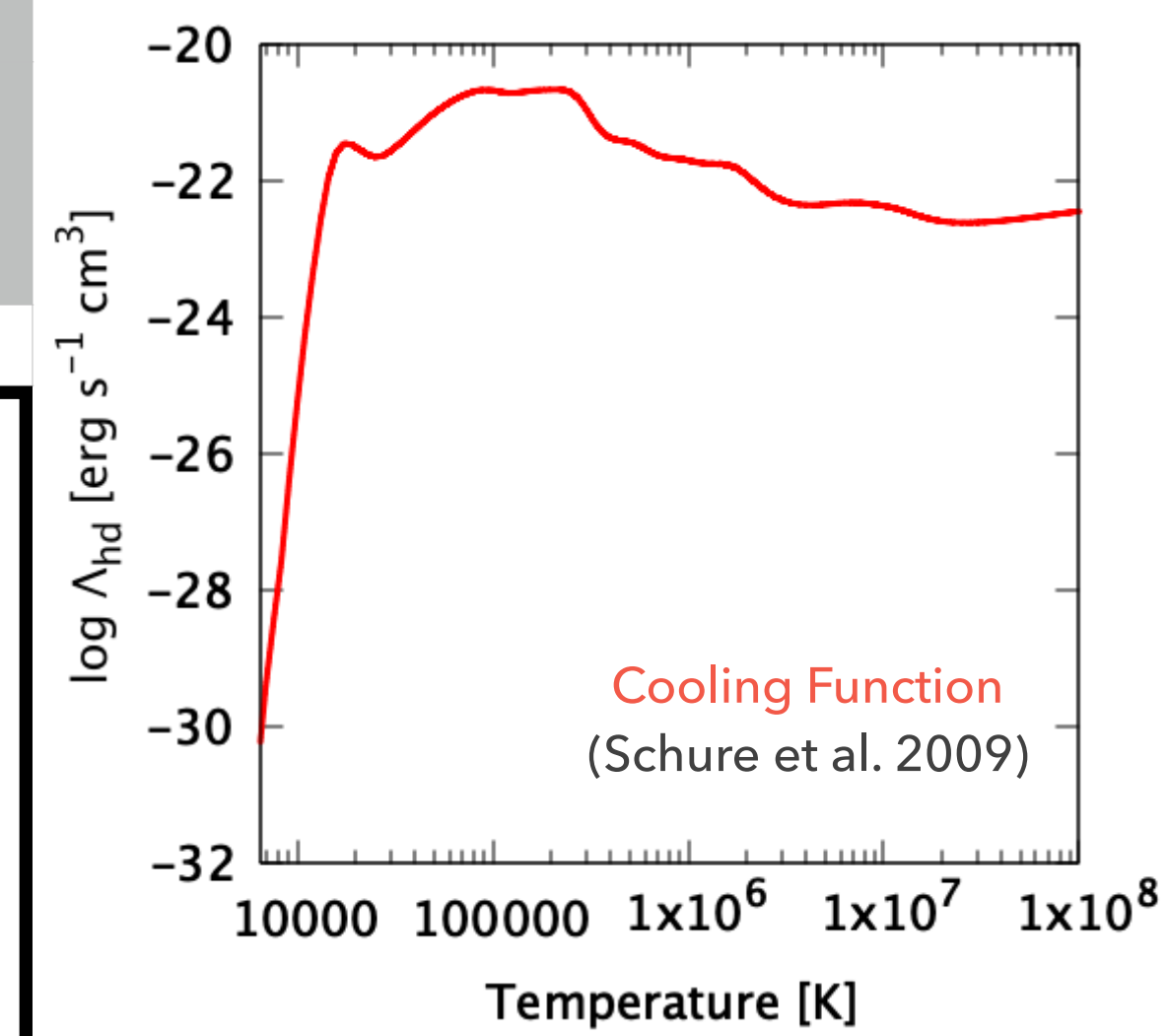
Radiative Cooling

(Saladino et al. 2018)

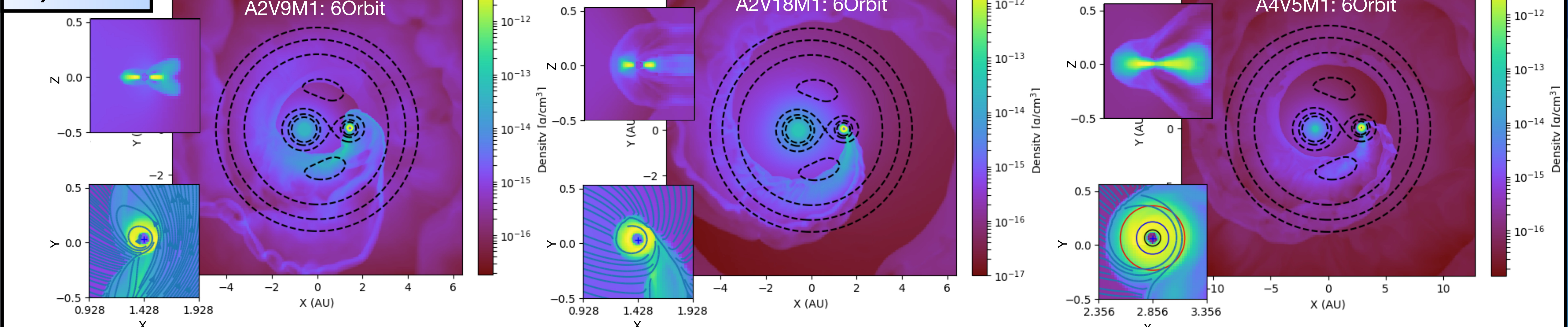
Equation of State

$$P = K\rho^\gamma \quad \gamma = 5/3$$

Ṁ = Mass loss rate
v_w = Wind velocity
f = Reduced G. factor
r_{soft1,2} = Softening radii
T_{eq} = Equilibrium temperature (Bowen 1988)
C = Recombination time scale
Λ_{hd} = Radiative cooling rate (Schure et al. 2009)



3.1) Results



A2V9M1

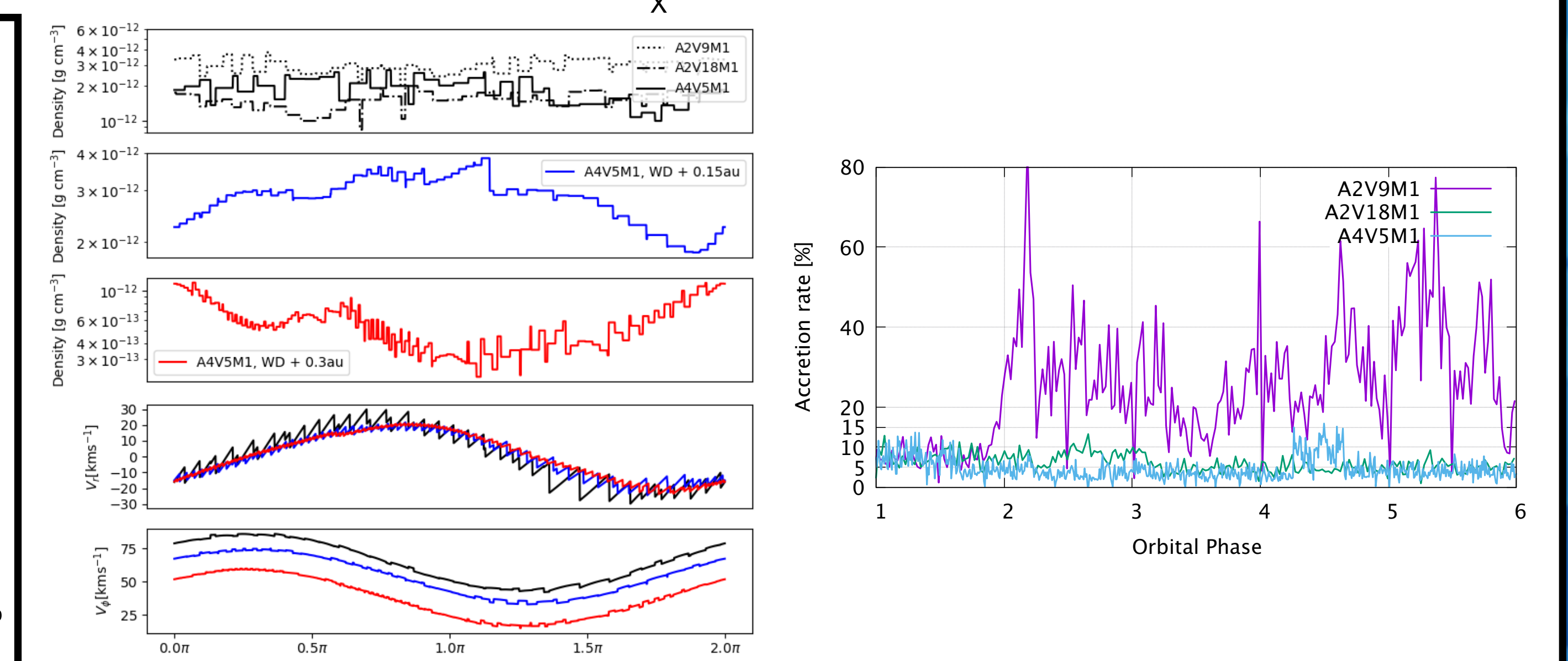
- Diffusive, eccentric accretion disk is formed during all of the simulation.
- Three main streams (wind, bow shock front and accretion wake) feed the accretion disk.
- Disk eccentricity is induced by high pressure in the accretion wake (which is in contrast to the result of Huarte-Espinoza et al. 2013).
- The bow shock stand-off distance is affected by bounded overshooted wake, and quasiperiodic accretion pattern.

A2V18M1

- Ram pressure balancing is achieved by the fast stellar wind.
- Bow shock stand-off distance is much shorter than A2V9M1.
- Compared to A2V9M1, inter-arm distance is increased by a factor of ~2.
- A sufficient radiative cooling produces a narrow bow shock front.
- Quasiperiodic accretion pattern, such as A2V9M1, is not shown in this model.
- Accretion rate converges to ~ 5%.

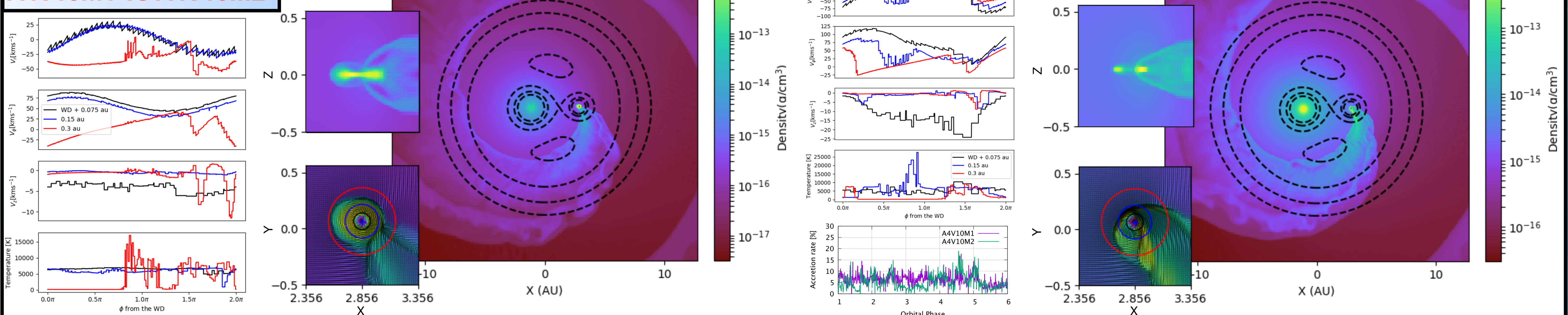
A4V5M1

- The widest, thin accretion disk in this study is formed.
- The main region of disk (blue solid lines in the right panels) show asymmetry in density.
- Rotational velocity, V_φ, tends to be faster at the incoming side of disk (0 < φ < 0.5π & 1.5π < φ < 2π) due to the inflow fluid from the accretion wake.
- Accretion rate converges to ~ 5%.



3.2) The role of Ṁ :

A4V10M1 vs A4V10M2



A4V10M1

- Relatively low pressure $[P_{1,2} \propto \rho_{1,2}^\gamma = (\dot{M}_{1,2} / 4\pi r^2 v_w)^\gamma]$ in the vicinity of the WD induces compression in the equatorial plane leading to the formation of an accretion disk.
- Slower radial velocity (V_r, compare to A4V10M2) also enhances stabilization of the accretion flow.
- Thermal equilibrium appears to be achieved in the accretion disk.

A4V10M2

- Enhanced density field generates massive accretion wakes, prohibiting the formation of an accretion disk due to the violent accretion wake.
- Radial and rotational velocities, which are much higher than A4V10M1, also support the violent feeding.
- Quasiperiodic accretion patterns are exhibited in both A4V10M1 and A4V10M2.

The role of Ṁ

- From our experimental models (A2V9M2, A2V18M2 and A4V5M1, not shown in this poster), the wind velocity play a more important role rather than the mass loss rate of the giant.
- This implies accretion rates may be insensitive to the mass loss rate of giant when the wind velocity is fixed.
- The pressure threshold may exist which will provide a criterion for formation of an accretion disk ($P_{1,2} \propto \rho_{1,2}^\gamma$: Accretion disk is formed, $P_{1,2} < P_{1,2}^\gamma$: Accretion disk is not formed).

4) Summary

- We find that three main streams (direct stream from the giant, stream following the accretion wake, and stream passing through the bow shock front) feed the disk and that general properties of accretion disks are closely related to wake overshooting and re-capturing processes.
- Our simulations show that accretion disks tend to be asymmetric due to the accretion wake feeding. We also observe the asymmetry, eccentricity and quasiperiodic accretion patterns that are affected by ram pressure balancing between wake and wind.
- By comparing A4V10M1 with A4V10M2, we propose that the pressure threshold may be present leading to formation of an accretion disk.